IEEE Access
Multidisciplinary : Rapid Review : Open Access Journal

Received December 17, 2018, accepted January 7, 2019, date of publication January 16, 2019, date of current version February 6, 2019.

Digital Object Identifier 10.1109/ACCESS.2019.2892509

Power Factor Control Method Based on Virtual Capacitors for Three-Phase Matrix Rectifiers

JAE-CHANG KIM[1], SANGSHIN KWAK[1], (Member, IEEE), AND TAEHYUNG KIM[2], (Senior Member, IEEE)
[1]School of Electrical and Electronics Engineering, Chung-Ang University, Seoul 156-756, South Korea
[2]Electrical and Computer Engineering Department, University of Michigan-Dearborn, Dearborn, MI 48128, USA

Corresponding author: Sangshin Kwak (sskwak@cau.ac.kr)

This work was supported by the National Research Foundation of Korea (NRF) through the Korean Government (MSIP) under Grant 2017R1A2B4011444.

ABSTRACT This paper proposes a novel input power factor control method based on a concept of virtual capacitors to provide unity input power factor for three-phase matrix rectifiers. The proposed algorithm introduces, at the input terminal of the matrix rectifier, an imaginary input capacitor generated by modifying a reference vector of the space vector modulation method. The virtual input capacitor, which is fictitiously built in parallel with an input LC filter, successfully compensates for the leading power factor of the LC filter of the matrix rectifier. Thus, the proposed method yields a unity power factor operation despite the presence of the LC filter of the three-phase matrix rectifier. In addition, under a condition when the unity power factor operation cannot be realized, the proposed algorithm adjusts a virtual capacitance to obtain a maximum achievable power factor operation. Because the proposed technique yields the input power factor control by introducing the virtual capacitor and adjusting a reference space vector, the proposed algorithm can be easily incorporated with conventional space vector modulation algorithms for the three-phase matrix rectifiers. Thus, the proposed method can control input power factor without employing proportional–integral controllers used in conventional power factor control methods for the matrix rectifiers, leading to simple control structure and straightforward tuning process for power factor control.

INDEX TERMS Matrix rectifier, power factor control, virtual capacitor.

I. INTRODUCTION

Recently, research on ac-to-dc power converters for energy storage devices such as batteries have increased with the increasing penetration of renewable energy systems into electrical grids [1]–[4]. Voltage source converters (VSCs) have been mainly used for charging batteries from grid systems, due to the unity power factor operation, sinusoidal source currents with high quality, and bidirectional power flow capability [5]. Because of the boosting characteristics of the VSC, an additional dc to dc converter is in general required to charge batteries having a rated voltage less than a peak voltage value of ac grids, yielding a two-stage power conversion structure with the VSC and the dc to dc converter [6]. On the other hand, ac to dc matrix rectifiers characterized by a current source converter, derived from well-known ac-to-ac matrix converters, are featured as a buck-type converter, which produces the dc output voltage lower than the peak value of ac source voltages [7]–[10]. As a result, the matrix rectifier can directly link the ac source to the battery charging systems with no employment of additional dc-to-dc converters, which can lead to a single-stage power conversion. Furthermore, the matrix rectifiers generate sinusoidal source currents as well as bidirectional power flow ability [11].

The most popular modulation algorithm for the matrix rectifier is the space vector modulation (SVM) method to synthesize sinusoidal source currents [11], [12]. On the other hand, the matrix rectifier is equipped with an LC filter on its input terminal for the purpose of commutations of switching devices and harmonic filtering, similar to current source converters. However, currents flowing through the input capacitor of the LC filter yield a phase difference between the source voltage and the source current, resulting in a reduced input power factor. Thus, several researches for the matrix rectifiers and the current source converters have been conducted to control the input power factor to unity or a maximum achievable power factor (MAPF) by compensating the effects of the input capacitor currents on the phase difference [13]–[16]. The techniques to control the input power factor of the matrix rectifier operated by the SVM algorithm were mostly developed by changing modulation index and delay angle using proportional–integral (PI) controllers assigned to adjust the modulation index control and the delay angle control [13], [14], [15]. In [16], the power factor control method based on a platform of the model predictive direct power control method was developed to adjust the input power factor. Although this method successfully improved the input power factor, the model predictive control method is exposed to a disadvantage of varying switching frequency, different from the SVM based method. Thus, most of power factor control approaches for the matrix rectifiers with the SVM are based on PI controllers, which are exposed to difficult tuning processes for power factor control.

This paper proposes a novel input power factor control method based on the concept of virtual capacitance, to provide unity input power factor for three-phase matrix rectifiers operated by the SVM method. The proposed algorithm introduces, at the input terminal of the matrix rectifier, an imaginary input capacitor generated by modifying a reference vector of the SVM method. The virtual input capacitor, which is fictitiously built in parallel with an input LC filter, successfully compensates for the leading power factor of the LC filter of the matrix rectifier. Thus, the proposed method yields a unity power factor operation despite the presence of the LC filter of the three-phase matrix rectifier. In addition, under conditions when the unity power factor operation cannot be realized at light loads, the proposed algorithm adjusts a virtual capacitance to obtain a MAPF operation. Therefore, the unity power factor or the MAPF operation can be accomplished under the given conditions. Because the proposed technique yields the input power factor control by introducing the virtual capacitor and adjusting a reference space vector, the proposed algorithm can be easily incorporated with conventional SVM algorithms for the three-phase matrix rectifiers. Thus, the proposed method can control input power factor without employing PI controllers used in conventional power factor control methods for matrix rectifiers, leading to simple control structure and straightforward tuning process for power factor control. The effectiveness of the proposed input power factor control technique is verified by simulations and experiments.

II. MATRIX RECTIFIER AND SPACE VECTOR MODULATION

Fig. 1 shows a topology of the matrix rectifier, where v_{sa}, i_{sa}, and i_{wa} represent *a*-phase source voltage, *a*-phase source current, and *a*-phase converter input current, respectively. In addition, L_f denotes the input inductor, and C_f is the input capacitor in the input LC filter of the matrix rectifier. Furthermore, L_o and C_o symbolize the output inductor and the output capacitor, respectively. I_{dc} signifies the dc current of the output LC filter, I_{load} denotes the dc load current, and V_{load} is the dc load voltage. The six bidirectional switches of

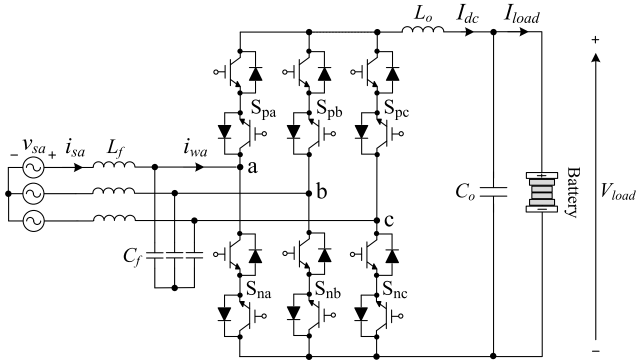

FIGURE 1. Matrix rectifier.

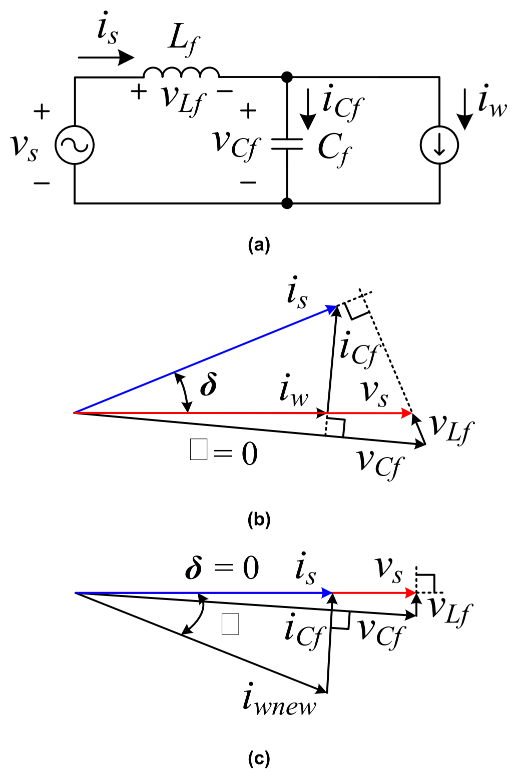

FIGURE 2. (a) Per-phase equivalent circuit of input part of matrix rectifier, (b) vector diagram in case of nonunity input power factor, and (c) vector diagram in case of unity input power factor.

the matrix rectifier are represented by S_{pa}, S_{pb}, S_{pc}, S_{na}, S_{nb}, and S_{nc}.

The input LC filter is installed at the input terminals of the matrix rectifier to remove harmonics of the converter input currents and generate sinusoidal source currents. However, this LC filter makes the phase difference between the source voltage and the source current, due to input capacitor currents, which deviates the input power factor from unity. A per-phase equivalent circuit of the input part of the matrix rectifier is shown by Fig. 2 (a). As seen in Fig. 2, v_{Lf} is the voltage across the input inductor and v_{Cf} denotes the voltage across the input capacitor. i_{Cf} is the current flowing through the input capacitor. Fig. 2 (b) is a vector diagram showing the relationship between the voltage and the current at the fundamental frequency in Fig. 2 (a). As shown in Fig. 2 (b), due to the input capacitor current i_{Cf}, the input power factor angle between the source voltage and the source current, denoted by δ occurs. A vector diagram in a case when the matrix rectifier operates at unity power factor, by nullifying the phase difference δ, is shown in Fig. 2 (c), in which ϕ, called a delay angle, is the angle between the input voltage and the converter input current. By comparing Fig. 2 (b) and (c), it can be seen that the delay angle and the magnitude of the converter input current obtained from Fig. 2 (c) are increased compared with those from Fig. 2 (b). The increments lead to unity power factor by making the input power factor angle δ zero, with the output voltage regulated. This relationship can be confirmed by (1).

$$V_{load} = 1.5 V_s m_i \cos\phi. \tag{1}$$

$$m_i = \frac{I_{w1}}{I_{dc}} \cdot (0 \leq m_i \leq 1) \tag{2}$$

where m_i, I_{w1}, and V_s denote the modulation index, the peak value of the fundamental component of i_w, and the peak value of the source voltage, respectively. From the vector diagrams of Figs. 2 (b) and (c), it can be seen that the delay angle ϕ should be increased to improve the input power factor. In addition, from (1), to keep the constant load voltage, it can be known that the decrease of cos ϕ due to the increase of the delay angle ϕ should be compensated by the increase of the modulation index, which leads to increased converter input current as shown in (2). As a result, the increased converter input current and the delay angle are required for the unity power factor operation in the matrix rectifier.

TABLE 1. Switching states and space vector of input currents in matrix rectifier.

	On-state switch	Converter input current			Space vector
		i_{wa}	i_{wb}	i_{wc}	
Active states	S_{pa}, S_{nb}	I_{dc}	$-I_{dc}$	0	I_1
	S_{pa}, S_{nc}	I_{dc}	0	$-I_{dc}$	I_2
	S_{pb}, S_{nc}	0	I_{dc}	$-I_{dc}$	I_3
	S_{pb}, S_{na}	$-I_{dc}$	I_{dc}	0	I_4
	S_{pc}, S_{na}	$-I_{dc}$	0	I_{dc}	I_5
	S_{pc}, S_{nb}	0	$-I_{dc}$	I_{dc}	I_6
Zero states	S_{pa}, S_{na}	0	0	0	I_0 (I_7)
	S_{pb}, S_{nb}				I_0 (I_8)
	S_{pc}, S_{nc}				I_0 (I_9)

The SVM method is the most common method for controlling the matrix rectifier. Six active vectors and two zero vectors, which can be synthesized by switching states of the matrix rectifier, are summarized in Table 1. In the SVM method, two active vectors and one zero vector, depending on a location of a reference vector, are used during a sampling period to generate a reference vector of the converter input current. Fig. 3 is a space vector diagram of the input current vector of the matrix rectifier, where I_{ref} is the reference vector of the converter input current. The dwelling times of active and zero vectors can be obtained from the magnitude of the reference vector related to modulation index m_i and the location of the reference vector associated with angle θ.

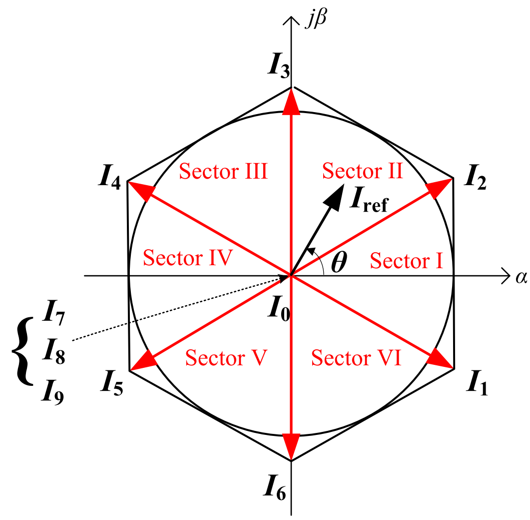

FIGURE 3. Space vector diagram of input current vector for matrix rectifier.

III. PROPOSED METHOD

A. VIRTUAL CAPACITOR-BASED POWER FACTOR CONTROL ALGORITHM

The current flowing into the input capacitor results in the source current out of phase with the source voltage, yielding a nonunity input power factor as shown in Fig. 2 (b). As a result, injecting a proper compensation current compensating for the input capacitor current i_{Cf} can improve the input power factor, leading to either unity input power factor, if possible, or maximum achievable power factor, in cases where unity power factor operation is not possible. Thus, a novel input power factor control algorithm based on a concept of a virtual capacitor is developed in this study. In the proposed method, the matrix rectifier generates an imaginary compensation current through a virtual capacitor, which is fictitiously set up in parallel with the input capacitor C_f. The resultant compensation current of the virtual capacitor can eliminate the phase difference between the source voltage and the source current, leading to input power factor improvement, despite the existence of input capacitors. Because the matrix rectifier can effectively eliminate the input capacitor current by generating the extra current with the opposite polarity with the input capacitor current, the additional current component of the matrix rectifier can be obtained using the input capacitor voltage and the negative value of the

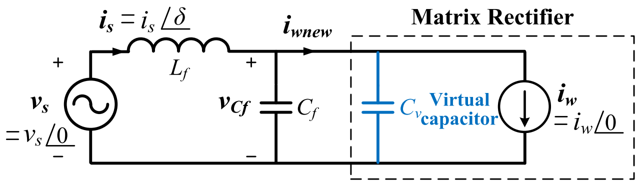

FIGURE 4. Equivalent circuit of proposed method based on virtual capacitor.

input capacitance. As a result, the capacitance of the virtual capacitor has the opposite polarity of the input capacitance as well as the extra current component of the rectifier for the input power factor adjustment has the opposite polarity of the input capacitor current. Fig. 4 shows an equivalent circuit of the matrix rectifier operating with the proposed power factor control method based on the virtual capacitor. Because the virtual capacitor is fictitiously placed in parallel with the input capacitor C_f, the current flowing through the virtual capacitor i_{Cv} is given by

$$i_{Cv} = C_v \frac{dv_{Cf}}{dt}, \tag{3}$$

where C_v is the capacitance of the virtual capacitor. The derivative of the voltage across the input capacitor v_{Cf} of (3) can be expressed as

$$\frac{dv_{Cf}}{dt} \approx \frac{v_{Cf}(k) - v_{Cf}(k-1)}{T_s}, \tag{4}$$

where $v_{Cf}(k)$ and $v_{Cf}(k-1)$ represent the capacitor voltage at the k^{th} and $(k-1)^{\text{th}}$ sampling instants, respectively.

It is desirable to filter out the harmonic components contained in the capacitor voltage v_{Cf} in the process of injecting the virtual capacitor current in (3) and (4), because only fundamental components are involved in the power factor control process. Because it is not easy to filter out harmonics and extract only fundamental 60 Hz components without harmonic components in general, a harmonic elimination technique using the dq transformation is used to remove the harmonics of the capacitor voltage. In the dq frame, dc components, which are the fundamental component in the abc frame, can be easily obtained by a low-pass filter (LPF). The harmonic elimination technique using the dq conversion is as follows. First, the result of abc-to-dq conversion of the measured three-phase capacitor voltage is passed through the LPF with a low cut-off frequency. Here, the dc value obtained by passing through the LPF is the fundamental frequency component. Then, dq-to-$\alpha\beta$ conversion is performed using the output value of the LPF. From the fundamental frequency component of the input capacitor voltage and (3), the currents $i_{Cv\alpha}$ and $i_{Cv\beta}$ without harmonic contaminations that flow through the virtual capacitor in the $\alpha\beta$ axis can be obtained. The virtual capacitor current for the input power factor adjustment is added to a reference current vector for the SVM method. Thus, a new reference current vector i^*_{wnew} for the SVM block in the proposed method includes a reference current component i^*_w for the output current control and a virtual capacitor current component i_{Cv} for the input power factor control. Here, the output current control component i^*_w is calculated by using the modulation index m_i, dc output current I_{dc}, and phase angle of the input voltage θ. The three-phase reference current is expressed by (5). The subscripts a, b, and c in (5) symbolize a-phase, b-phase, and c-phase respectively.

$$\begin{aligned} i^*_{wa} &= m_i I_{dc}\cos(\theta) \\ i^*_{wb} &= m_i I_{dc}\cos(\theta - \frac{2\pi}{3}) \\ i^*_{wc} &= m_i I_{dc}\cos(\theta + \frac{2\pi}{3}). \end{aligned} \tag{5}$$

In (5), the modulation index m_i is obtained by the output of the PI controller for output current control and I_{dc} is achieved by the measurement of the dc output current. The reference currents for the output current control, $i^*_{w\alpha}$ and $i^*_{w\beta}$, in the $\alpha\beta$ axis can be obtained by abc-to-$\alpha\beta$ transformation by using (6). The output current control component and the virtual capacitor current component are added to obtain the new reference current vector as shown in (7).

$$\begin{bmatrix} i^*_{w\alpha} \\ i^*_{w\beta} \end{bmatrix} = \frac{2}{3}\begin{bmatrix} 1 & -\frac{1}{2} & -\frac{1}{2} \\ 0 & \frac{\sqrt{3}}{2} & -\frac{\sqrt{3}}{2} \end{bmatrix}\begin{bmatrix} i^*_{wa} \\ i^*_{wb} \\ i^*_{wc} \end{bmatrix}. \tag{6}$$

$$\begin{aligned} i^*_{wnew\alpha} &= i^*_{w\alpha} + i_{Cv\alpha} \\ i^*_{wnew\beta} &= i^*_{w\beta} + i_{Cv\beta}. \end{aligned} \tag{7}$$

Since the modulation Index and the phase angle are required to control the rectifier using the SVM method, a modulation index m_{inew} and a phase angle θ_{new} from the new reference current vector i^*_{wnew} are calculated as follows.

$$m_{inew} = \frac{\sqrt{(i^*_{wnew\alpha})^2 + (i^*_{wnew\beta})^2}}{I_{dc}}. \tag{8}$$

$$\theta_{new} = \tan^{-1}(\frac{i^*_{wnew\beta}}{i^*_{wnew\alpha}}). \tag{9}$$

Fig. 5 shows the overall block diagram of the proposed power factor control method based on the virtual capacitor. From Fig. 5, it is known that the proposed algorithm uses a straightforward tuning process of input power factor control for the matrix rectifier, without the complicated tuning process of PI controllers, leading to a simple power factor adjustment algorithm.

B. MAXIMUM ACHIEVABLE POWER FACTOR

As shown in Figs. 2 (b) and (c), the matrix rectifier adjusts the input power factor by increasing the converter input current and the delay angle. However, as can be seen from (1) and (2), under conditions of light load with small I_{dc}, the converter input current and the delay angle cannot be increased enough to achieve unity power factor, because the modulation index is limited to be less than one and the output voltage should be kept constant. As a result, in cases that the matrix converter

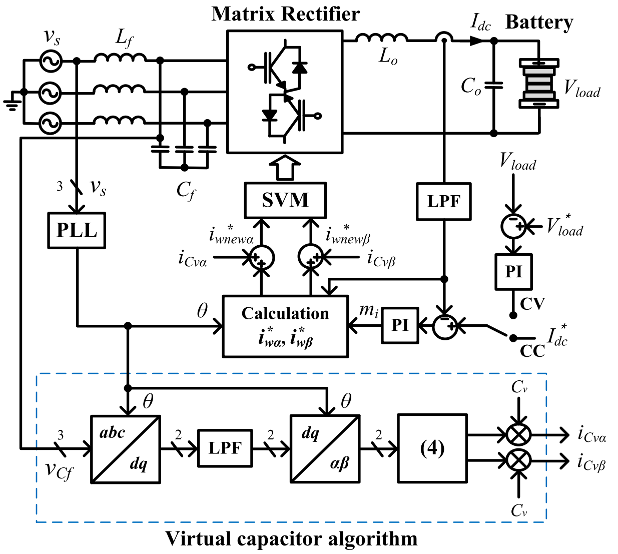

FIGURE 5. Overall block diagram of the proposed method.

operates at light loads, it can only work at the maximum achievable power factor (MAPF), instead of at unity power factor. Operation conditions depending on the maximum value of the virtual capacitance and the corresponding MAPF are investigated in this subsection.

From Fig. 4, the source current and the input power factor of the matrix rectifier can be derived using the virtual capacitance as follows:

$$\boldsymbol{i_s} = \frac{i_w + j\omega V_s(C_f + C_v)}{1 - \omega^2 L_f(C_f + C_v)}. \tag{10}$$

$$\cos(\delta) = \cos(\tan^{-1}(\frac{\omega V_s(C_f + C_v)}{i_w})). \tag{11}$$

From (11), it can be seen that unity power factor can be obtained when the virtual capacitance generated by the matrix rectifier nullifies the input capacitance. However, at light loads, the matrix rectifier cannot generate additional input currents enough to *emulate* the virtual capacitance canceling the input capacitance, leading to MAPF conditions instead of unity power factor operations.

Let us notate the maximum value of the virtual capacitance that can be generated by the matrix rectifier under a given circuit and load condition by $C_{v\max}$. In cases when the maximum virtual capacitance $C_{v\max}$ is bigger than the input capacitance C_f, the matrix rectifier can operate at unity power factor. In contrast, when $C_{v\max}$ is smaller than C_f, the MAPF operation should be obtained, rather than the unity power factor operation. Since the new modulation index m_{inew} increases as the magnitude of the capacitance of the virtual capacitor increases as seen from (3), (7), and (8), the virtual capacitance reaches a maximum value when m_{inew} becomes one.

From Fig. 4, the new converter input current vector $\boldsymbol{i_{wnew}}$ that includes the virtual capacitor current vector can be calculated as follows:

$$\boldsymbol{i_{wnew}} = \frac{1 - \omega^2 L_f C_f}{1 - \omega^2 L_f(C_f + C_v)}(i_w + j(\frac{\omega C_v V_s}{1 - \omega^2 L_f C_f})). \tag{12}$$

The condition to achieve the maximum virtual capacitance can be determined from (12) and with $m_{inew} = 1$ and leads to (13).

$$|i_{wnew}| = \frac{1 - \omega^2 L_f C_f}{1 - \omega^2 L_f(C_f + C_{v\max})}\sqrt{(i_w)^2 + (\frac{\omega C_{v\max} V_s}{1 - \omega^2 L_f C_f})^2} = I_{dc}. \tag{13}$$

Solving (13) yields the maximum value of the virtual capacitance obtained by the matrix rectifier as follows.

$$C_{v\max} = \frac{-k_2 \pm \sqrt{(k_2)^2 - 4k_1(k_3)^2((i_w)^2 - (I_{dc})^2)}}{2k_1}. \tag{14}$$

where

$$k_1 = \omega^2(V_s)^2 - \omega^4(L_f)^2(I_{dc})^2$$
$$k_2 = 2(1 - \omega^2 L_f C_f)\omega^2 L_s(I_{dc})^2$$
$$k_3 = 1 - \omega^2 L_f C_f$$
$$i_w = \frac{I_{dc}V_{load}}{1.5V_s}.$$

It should be noted that a negative value between two roots obtained by (14) becomes $C_{v\max}$, because the virtual capacitance should be negative to reduce or cancel an effect of the input capacitance C_f. If the magnitude of $C_{v\max}$ obtained by (14) is equal to or larger than the input capacitance C_f, the matrix rectifier can operate at unity input power factor, by setting $C_v = -C_f$. On the other hand, when the absolute value of the maximum virtual capacitance obtained using (14) is smaller than C_f, the matrix rectifier works at the MAPF, by using $C_v = C_{v\max}$ in the controller. Thus, the input power factor obtained by the proposed algorithm is given, according to the relationship between the input capacitance and the maximum virtual capacitance, by

$$\text{Input power factor} = \begin{cases} 1, & C_f \le |C_{v\max}| \\ \cos(\tan^{-1}(\frac{(C_f + C_{v\max})\omega V_s}{i_w})), & C_f > |C_{v\max}|. \end{cases} \tag{15}$$

Fig. 6 shows the input power factor of the matrix rectifier obtained by the proposed method versus output power P_o, which is expressed by (16). In addition, the input power factor achieved by the conventional method is also depicted in Fig. 6 for a purpose of comparison. Fig. 6 was obtained by (11), (14), and (15) and parameters used in Table 2. It can be seen from Fig. 6 that the proposed power factor control method based on the virtual capacitor, given the constraints, can result in unity power factor for the matrix rectifier with output power higher than 1.1 kW. On the other hand, on light load condition with output power less than 1.1 kW, the matrix rectifier operated by the proposed method yields the input power factor less than unity, as shown in Fig. 6. It is also confirmed from Fig. 6 that the input power factor obtained

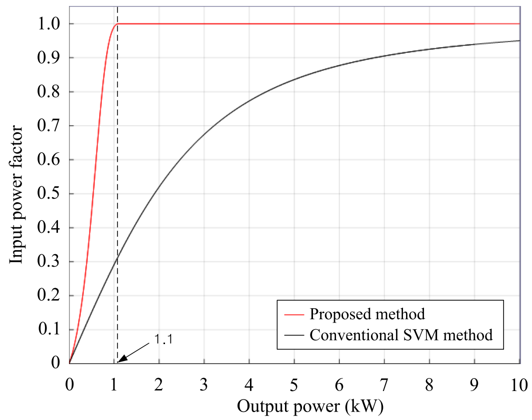

FIGURE 6. Input power factor obtained by proposed method and conventional SVM method, versus output power.

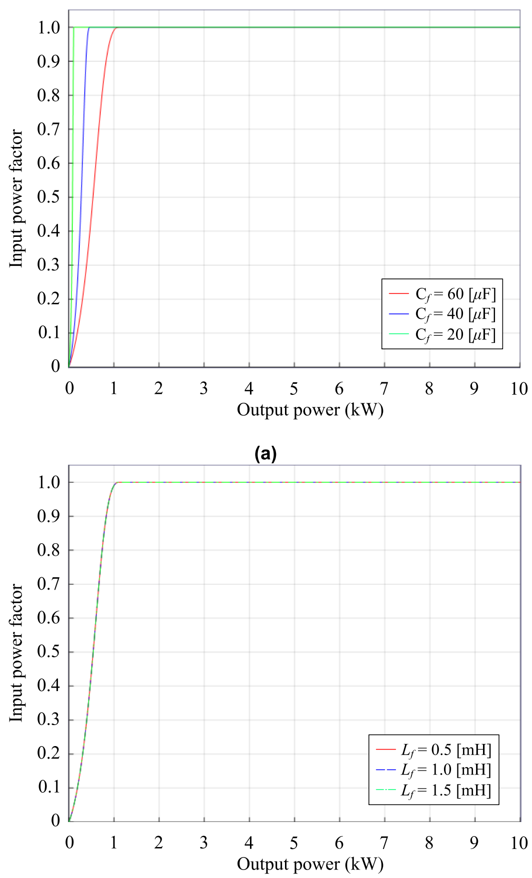

FIGURE 7. Input power factor as a function of output power with different (a) capacitances of the input capacitor and (b) inductances of the input inductor.

by the proposed method is much better than that of the conventional SVM method, for all load power ranges.

$$P_o = I_{dc} V_{load}. \tag{16}$$

Fig. 7 shows the plots of the input power factor as a function of output power with several values of the input filters, which are obtained by using (14) and (15), using the parameters in Table 2. Fig. 7 (a) shows the input power factor versus output power P_o with three input capacitances. From Fig. 7 (a), it is seen that with a fixed C_f, the matrix rectifier operates at MAPF at light loads with small P_o, instead of at unity power factor. In addition, as the input capacitance is decreased, the unity power factor is obtained with a lower output power, because the virtual capacitor current generated by the matrix rectifier, which should compensate for the current flowing through C_f, is reduced. Fig. 7 (b) shows the input power factor as a function P_o with three input inductances. From Fig. 7 (b), it can be seen that the input power factor of the matrix rectifier is not affected by the input inductance.

TABLE 2. Parameters for matrix rectifier.

Parameter	Value
Source phase voltage V_s	220 V_{rms}
Source voltage frequency f	60 Hz
Input inductance L_f	1 mH
Input capacitance C_f	60 μF
Output inductance L_o	2 mH
Output capacitance C_o	40 μF
Load resistance R	20 Ω
Sampling and switching frequency	5 kHz

IV. SIMULATION RESULTS

To verify the performance of the proposed method, simulations with parameters in Table 2 were performed, where the reference output current in simulations is 20 A.

Fig. 8 shows the simulation results of the conventional SVM method and the proposed method with the reference output current equal to 20 A. From Fig. 8 (a), in the matrix rectifier control by the conventional SVM method, the phase difference between the input source voltage and the input source current occurs due to the current flowing through the input capacitor. However, in the proposed method, as shown in Fig. 8 (b), the input power factor of the matrix rectifier is adjusted to unity, because the additional rectifier input current, which is the virtual capacitor current in the proposed algorithm, compensates for the input capacitor current.

Fig. 9 illustrates the simulation waveforms of the dc current in front of the output LC filter, the dc load voltage, and the dc load current from the conventional and the proposed methods. From Fig. 9, it can be known that the dc currents in the output LC filter generated by both the methods follow the reference value accurately. As a result, the dc load current passing through the output LC filter is controlled to be almost constant as shown. On the other hand, the ripples of the dc current I_{dc} obtained by the proposed method is smaller than those of the conventional method. This is because the ripple of the input current of the output LC filter of the matrix rectifier is proportional to the dwelling time of the zero-vector due

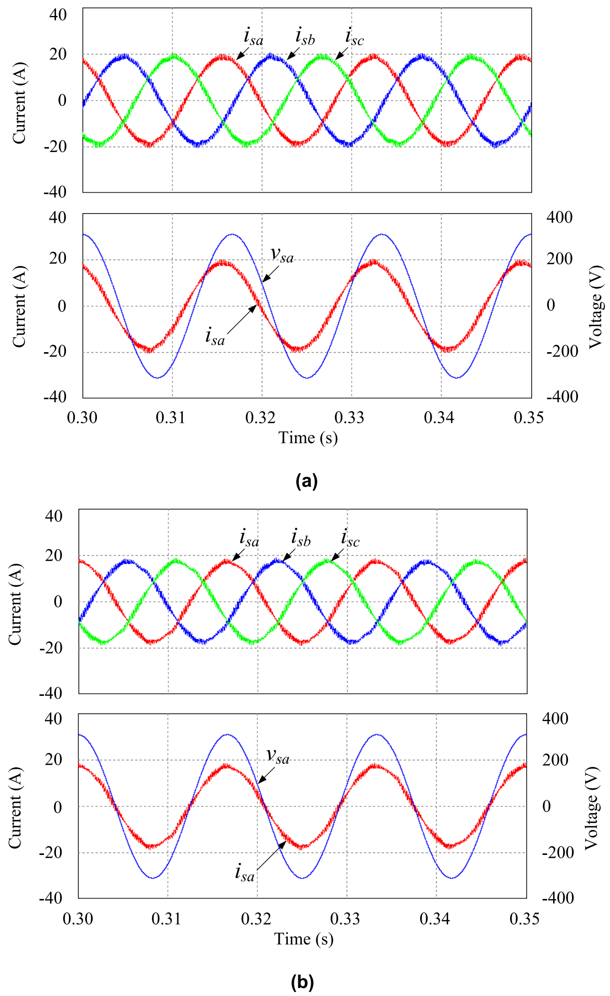

FIGURE 8. **Simulation results of the three-phase source currents and the *a*-phase input voltage of matrix rectifier obtained by (a) conventional SVM method and (b) proposed method.**

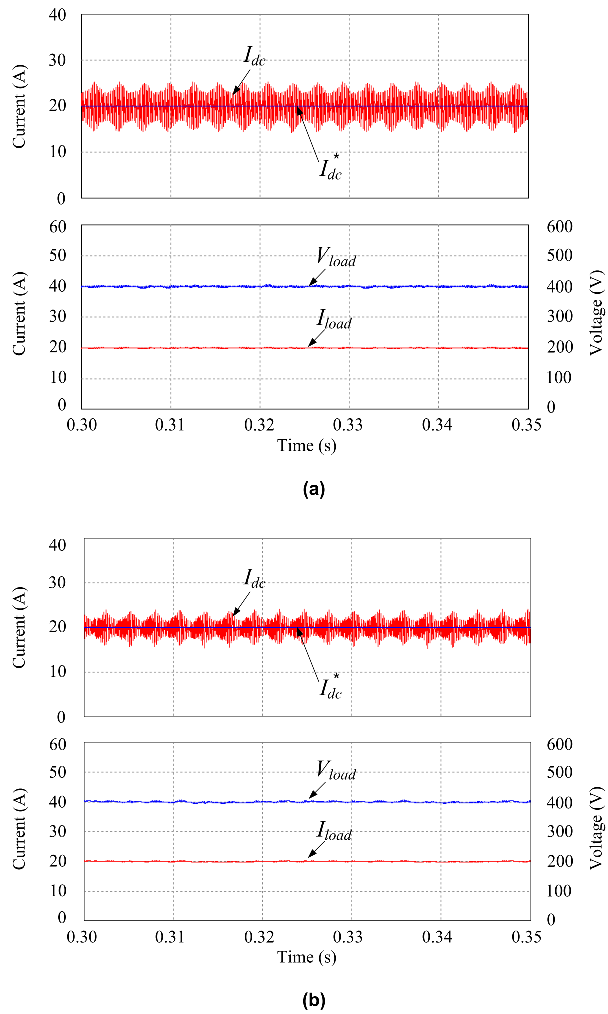

FIGURE 9. **Simulation results of dc current of output LC filter, load voltage, and load current obtained by (a) conventional SVM method and (b) proposed method.**

to the buck-type structure of the matrix rectifier, where the relationship between the fluctuation of the dc current of the output LC filter and the dwelling time of the zero-vector is expressed by [17] and [18]

$$\Delta I_{dc} = \frac{V_{load}}{L_o} T_o. \tag{17}$$

In the proposed method, the virtual capacitor current generated by the matrix rectifier for power factor control is added to the reference current for the SVM block, increasing the modulation index. This increased modulation index shortens the dwelling time of the zero-vector in the sampling period, in turn reducing the fluctuation of the dc current I_{dc}. From Fig. 8 and Fig. 9, it is seen that the proposed method generates the same load current and voltage as the conventional SVM method to deliver the same load power, whereas the magnitude of the source current of the proposed method is reduced in comparison with that of the conventional method due to the improved power factor.

Fig. 10 shows the simulation results of *a*-phase source current and *a*-phase source voltage at light load with the dc output current $I_{dc} = 6$ A, where the output power is 0.72 kW. As shown by the red line of Fig. 6, the load condition with the output power 0.72 kW corresponds to the MAPF operation, where the matrix rectifier cannot provide the unity power factor operation. For the MAPF operation, the maximum virtual capacitance for the proposed method is calculated by using (14). As shown in Fig. 10 (b) obtained from the proposed MAPF operation, although they are not in phase, the phase difference between the source voltage and the source current is greatly reduced in comparison with the conventional method shown in Fig. 10 (a). In addition, the source current produced by the proposed method is substantially decreased because of the improved input power factor, which can yield reduced conduction losses and higher efficiency, compared with the current in the conventional method. It should be noted that the proposed input power factor control method adjusts only the fundamental current component to shift the input power factor angle, whereas

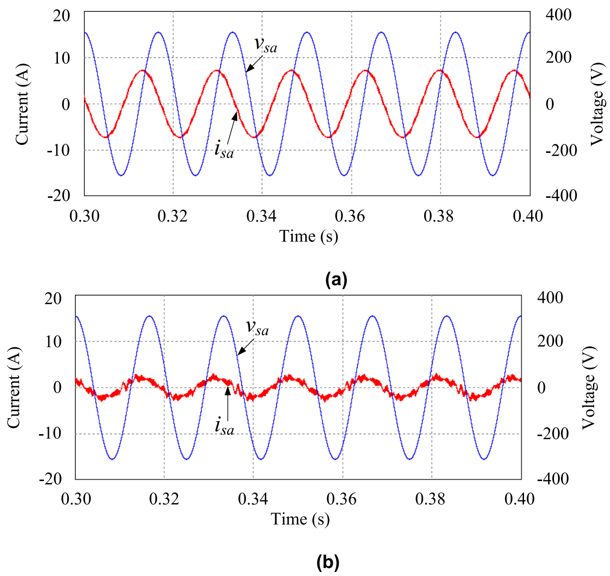

FIGURE 10. Simulation results of *a*-phase source current and *a*-phase source voltage under the MAPF condition at light load, obtained by (a) conventional SVM method and (b) proposed method.

harmonic current components remain intact, resulting in less sinusoidal source current waveform due to the reduced fundamental component. Fig. 10 illustrates that the proposed method works well under the MAPF operating conditions.

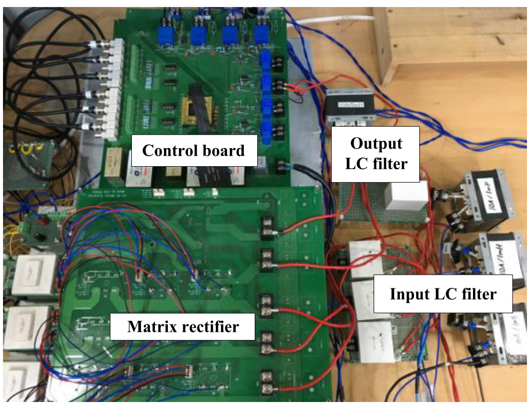

FIGURE 11. Experiment setup of three-phase matrix rectifier.

V. EXPERIMENT RESULTS

A prototype of the matrix rectifier was built in a laboratory with six bidirectional switches composed of insulated-gate bipolar transistor (IGBT) modules (SK80GM063) to verify the performance of the proposed power factor control method based on virtual capacitance. A Texas Instrument digital signal processor (DSP) board (TI TMS320F28335) was used to realize the SVM and the virtual capacitor-based power factor control scheme. Fig. 11 shows the prototype experiment setup. The parameters used in the experiment were the same as Table 2, except that the magnitude of the source voltage and the load resistance was 100 V and 18.5 Ω respectively.

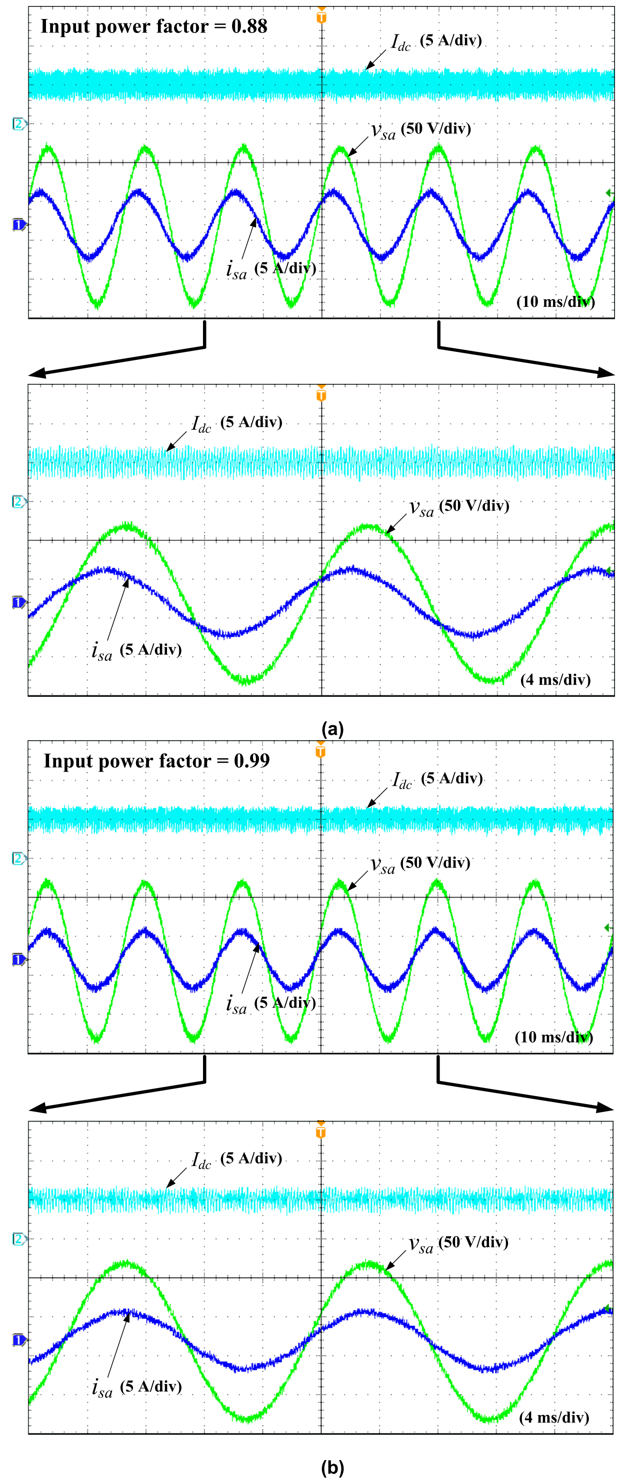

FIGURE 12. Experiment waveforms of *a*-phase source voltage, *a*-phase source current, and dc current of output LC filter obtained by (a) conventional SVM method and (b) proposed method.

Fig. 12 represents the experiment waveforms of the *a*-phase source voltage, *a*-phase source current, and dc current of the output LC filter obtained by the conventional method and the proposed method. Unlike existence of the phase difference between the source voltage and current in the conventional method, the proposed power factor control algorithm can generate the source current in phase with the source voltage, leading to unity power factor operation. As a result, the input power factor increases from 0.88 to 0.99 after applying the proposed algorithm. In addition, it can be seen from Fig. 12 that the magnitude of the source current of the proposed method is lower than that of the conventional method. Furthermore, it can be known that ripples of the dc current I_{dc} of the proposed method are reduced in comparison with the conventional method. Fig. 13 shows the experimental waveforms of the a-phase source voltage and the three-phase source currents obtained by the conventional SVM method and the proposed method.

Fig. 14 represents the experimental waveforms of the load current and the load voltage obtained by the conventional SVM method and the proposed method, where both the methods well regulate load current and voltage.

Fig. 15 represents the experiment waveforms of the a-phase source current and the a-phase source voltage at light load with the low dc output current $I_{dc} = 2$ A, which corresponds to the MAPF operation. Also, the detailed power factors were experimentally measured from the matrix rectifier operated by the conventional and the proposed method at light load, as shown in Fig. 15. The maximum virtual capacitance for the proposed method calculated by using (14) was used in the proposed method for the MAPF operation. The input power factor of the matrix rectifier with light load, obtained by the conventional and the proposed method, was 0.30 and 0.86, respectively. It is clearly seen from Fig. 15 that the measured input power factor of the rectifier controlled by the proposed method was increased to 0.86, whereas the power factor obtained by the conventional method was only 0.30. This is because the proposed method generates reduced phase angle between the source voltage and current in comparison with the conventional method, as shown the experimental waveforms in Fig. 15. As a consequence of the improved power factor, the source current of the rectifier operated by the proposed method contains much lower fundamental component and similar harmonic components than that by the conventional method. Thus, the proposed method can yield the input power factor better than the conventional method, although the source current waveform with decreased magnitude of the proposed method looks more distorted than that of the conventional method. It is seen that the source current produced by the proposed method has lower magnitude and has smaller phase difference with the source voltage than the conventional method. The decreased amplitude of the source current by the proposed power factor control algorithm can lead to reduced losses in power lines and improve efficiency.

Fig. 16 shows experiment results of frequency spectrum of a-phase source current obtained by the proposed method under both unity power factor condition and the MAPF condition at light load. As shown in Fig. 16 (a), the matrix rectifier operated by the proposed method leads to low total harmonic

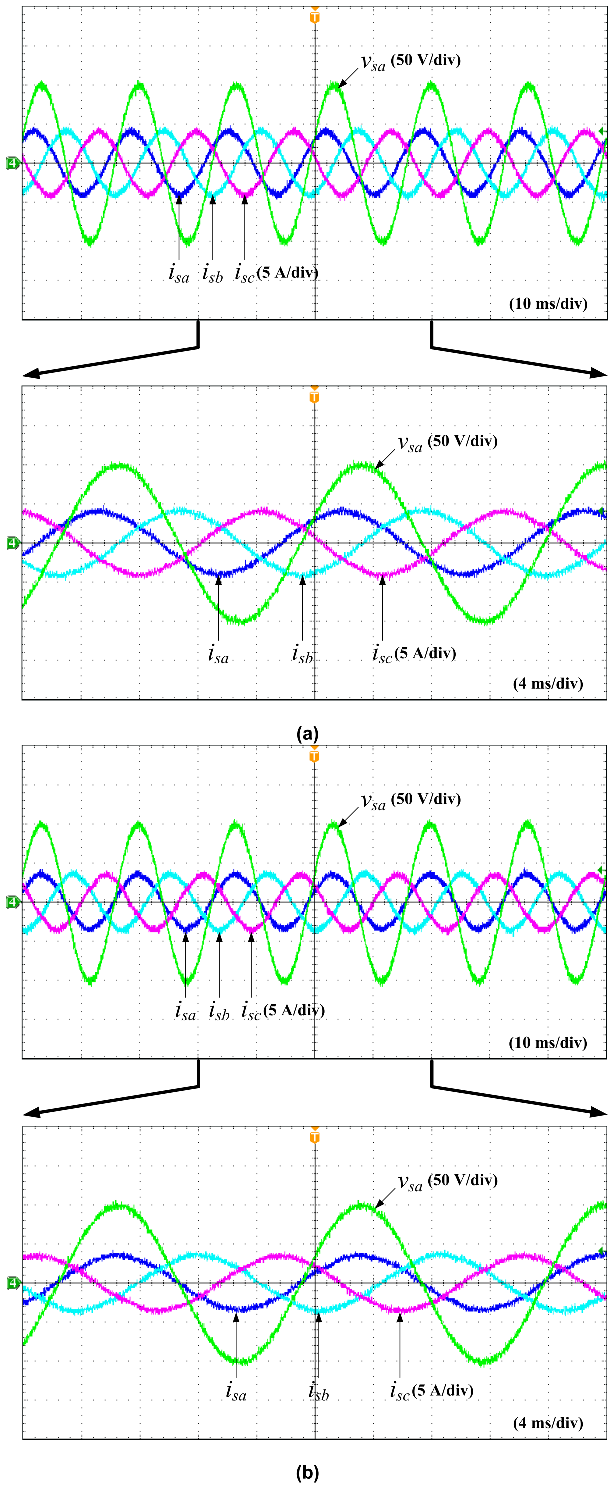

FIGURE 13. Experiment waveforms of a-phase source voltage and three-phase source currents obtained by (a) conventional SVM method and (b) proposed method.

distortion (THD) under unity power factor condition. On the other hands, under the MAPF condition at light load, the THD value of the source current is increased, mostly due to reduced fundamental component of the source current associated with

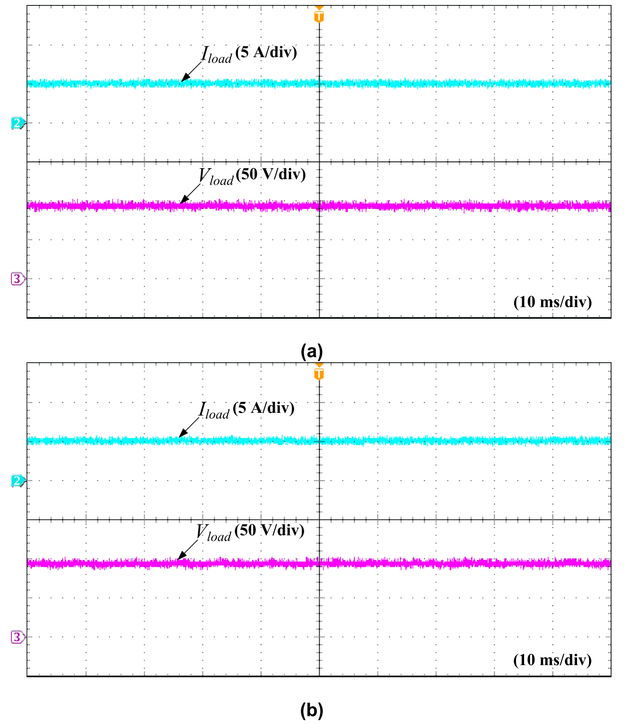

FIGURE 14. Experiment waveforms of load current and load voltage obtained by (a) conventional SVM method and (b) proposed method.

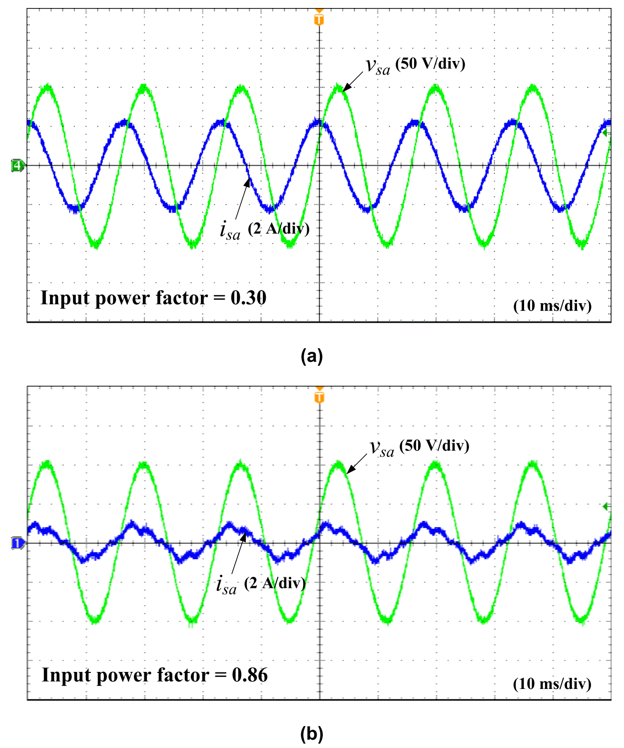

FIGURE 15. Experiment of *a*-phase source current and *a*-phase source voltage under the MAPF condition at light load, obtained by (a) conventional SVM method and (b) proposed method.

reduced phase angle between the source voltage and current, which resulted from input power factor improvement of the proposed method.

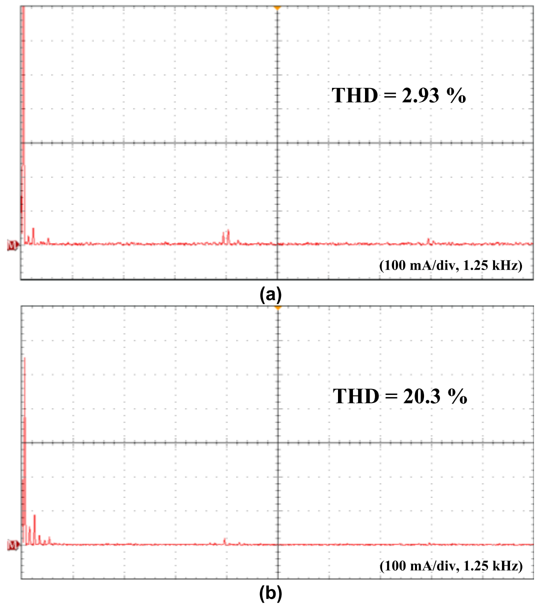

FIGURE 16. Experiment results of frequency spectrum of *a*-phase source current obtained by the proposed method under (a) unity power factor condition and (b) MAPF condition at light load.

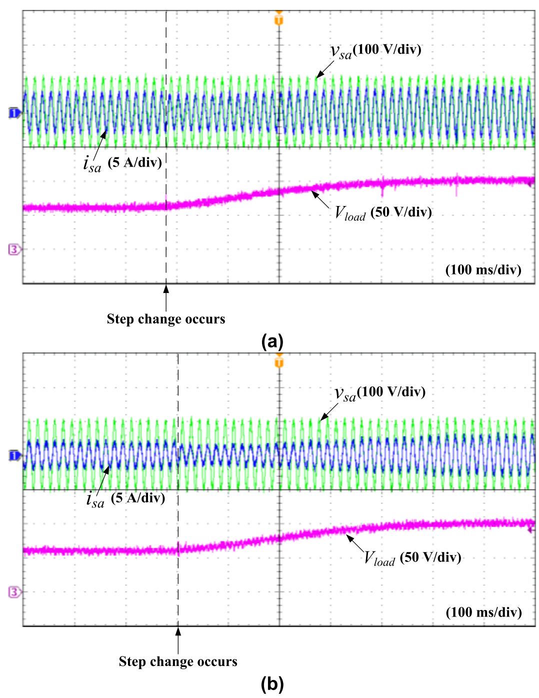

FIGURE 17. Experiment results of *a*-phase source voltage, *a*-phase source current, and load voltage when load step change occurs from 15 Ω to 25 Ω, obtained by (a) conventional SVM method and (b) proposed method.

Fig. 17 represents experiment results of *a*-phase source voltage, *a*-phase source current, and the load voltage with a load step change from 15 Ω to 25 Ω, obtained by the conventional SVM method and the proposed method. It is seen that the magnitude of the source current obtained by the proposed method is lower than that of the conventional method due to the input power factor improvement.

VI. CONCLUSION

This paper proposed a novel input power factor control method based on the concept of virtual capacitance, to provide unity input power factor for three-phase matrix rectifiers. The virtual input capacitor, which is fictitiously built in parallel with an input LC filter, successfully compensates for the leading power factor of the LC filter of the matrix rectifier. Thus, the proposed method yielded a unity power factor operation despite the presence of the LC filter of the three-phase matrix rectifier. In addition, under conditions when the unity power factor operation cannot be realized at light loads, the proposed algorithm adjusts a virtual capacitance to obtain a MAPF operation. Therefore, the unity power factor or the MAPF operation can be accomplished depending on the given conditions. Because the proposed technique yields the input power factor control by introducing the virtual capacitor and adjusting a reference space vector, the proposed algorithm can be easily incorporated with conventional SVM algorithms for the three-phase matrix rectifiers. Thus, the proposed method can control input power factor without employing PI controllers used in conventional power factor control methods for the matrix rectifiers, leading to simple control structure and straightforward tuning process for power factor control. The effectiveness of the proposed input power factor control technique was verified by simulations and experiments.

REFERENCES

[1] S. Vazquez, S. M. Lukic, E. Galvan, L. G. Franquelo, and J. M. Carrasco, ''Energy storage systems for transport and grid applications,'' *IEEE Trans. Ind. Electron.*, vol. 57, no. 12, pp. 3881–3895, Dec. 2010.

[2] M. Yilmaz and P. T. Krein, ''Review of battery charger topologies, charging power levels, and infrastructure for plug-in electric and hybrid vehicles,'' *IEEE Trans. Power Electron.*, vol. 28, no. 5, pp. 2151–2169, May 2013.

[3] F. A. Bhuiyan and A. Yazdani, ''Energy storage technologies for grid-connected and off-grid power system applications,'' in *Proc. IEEE Elect. Power Energy Conf. (EPEC)*, Oct. 2012, pp. 303–310.

[4] B. P. Roberts and C. Sandberg, ''The role of energy storage in development of smart grids,'' *Proc. IEEE*, vol. 99, no. 6, pp. 1139–1144, Jun. 2011.

[5] J. R. Rodriguez, J. W. Dixon, J. R. Espinoza, J. Pontt, and P. Lezana, ''PWM regenerative rectifiers: State of the art,'' *IEEE Trans. Ind. Electron.*, vol. 52, no. 1, pp. 5–22, Feb. 2005.

[6] N. M. L. Tan, T. Abe, and H. Akagi, ''Design and performance of a bidirectional isolated DC-DC converter for a battery energy storage system,'' *IEEE Trans. Power Electron.*, vol. 27, no. 3, pp. 1237–1248, Mar. 2012.

[7] D. G. Holmes and T. A. Lipo, ''Implementation of a controlled rectifier using AC-AC matrix converter theory,'' *IEEE Trans. Power Electron.*, vol. 7, no. 1, pp. 240–250, Jan. 1992.

[8] K. You and M. F. Rahman, ''Application of general space vector modulation approach of AC-AC matrix converter theory to a new bidirectional converter for ISA 42 V system,'' in *Proc. Conf. Rec. 41st IEEE IAS Annu. Meeting*, vol. 5, Oct. 2006, pp. 2480–2487.

[9] K. You and M. F. Rahman, ''Modulations for three-phase AC-DC voltage source rectification and DC-three-phase AC voltage source inversion using general direct space vector approach,'' in *Proc. IEEE IECON*, Paris, France, Nov. 2006, pp. 2781–2786.

[10] K. You, D. Xiao, M. F. Rahman, and M. N. Uddin, ''Applying reduced general direct space vector modulation approach of AC–AC matrix converter theory to achieve direct power factor controlled three-phase AC–DC matrix rectifier,'' *IEEE Trans. Ind. Appl.*, vol. 50, no. 3, pp. 2243–2257, May/Jun. 2014.

[11] P. W. Wheeler, J. Rodriguez, J. C. Clare, L. Empringham, and A. Weinstein, ''Matrix converters: A technology review,'' *IEEE Trans. Ind. Electron.*, vol. 49, no. 2, pp. 276–288, Apr. 2002.

[12] J. Rodríguez, M. Rivera, J. W. Kolar, and P. W. Wheeler, ''A review of control and modulation methods for matrix converters,'' *IEEE Trans. Ind. Electron.*, vol. 59, no. 1, pp. 58–70, Jan. 2012.

[13] Y. Xiao, B. Wu, S. C. Rizzo, and R. Sotudeh, ''A novel power factor control scheme for high-power GTO current-source converter,'' *IEEE Trans. Ind. Appl.*, vol. 34, no. 6, pp. 1278–1283, Nov./Dec. 1998.

[14] N. R. Zargari, Y. Xiao, and B. Wu, ''Near unity input displacement factor for current source PWM drives,'' *IEEE Ind. Appl. Mag.*, vol. 5, no. 4, pp. 19–25, Jul. 1999.

[15] B. Feng, H. Lin, and X. Wang, ''Modulation and control of AC/DC matrix converter for battery energy storage application,'' *IET Power Electron.*, vol. 8, no. 9, pp. 1583–1594, 2015.

[16] H. Gao, B. Wu, D. Xu, and N. R. Zargari, ''A model predictive power factor control scheme with active damping function for current source rectifiers,'' *IEEE Trans. Power Electron.*, vol. 33, no. 3, pp. 2655–2667, Mar. 2018.

[17] B. Feng, H. Lin, X. Wang, X. An, and B. Liu, ''Optimal zero-vector configuration for space vector modulated AC-DC matrix converter,'' in *Proc. IEEE ECCE*, Raleigh, NC, USA, Sep. 2012, pp. 291–297.

[18] M. Su, H. Wang, Y. Sun, J. Yang, W. Xiong, and Y. Liu, ''AC/DC matrix converter with an optimized modulation strategy for V2G applications,'' *IEEE Trans. Power Electron.*, vol. 28, no. 12, pp. 5736–5745, Dec. 2013.

JAE-CHANG KIM received the B.S. degree in electrical and electronics engineering from Chung-Ang University, Seoul, South Korea, in 2017, where he is currently pursuing the combined M.S and Ph.D. degrees in electrical and electronics engineering. His research interests include control and analysis for two-level, multilevel, and matrix converters.

SANGSHIN KWAK (S'02–M'05) received the Ph.D. degree in electrical engineering from Texas A&M University, College Station, TX, USA, in 2005. From 1999 to 2000, he was a Research Engineer with LG Electronics, Changwon, South Korea. He was also with Whirlpool R&D Center, Benton Harbor, MI, USA, in 2004. From 2005 to 2007, he was a Senior Engineer with Samsung SDI R&D Center, Yongin, South Korea. From 2007 to 2010, he was an Assistant Professor with Daegu University, Gyeongsan, South Korea. Since 2010, he has been with Chung-Ang University, Seoul, South Korea, where he is currently a Professor. His research interests include topology design, modeling, modulation, and control of power converters, multilevel converters, renewable energy systems, and power quality.

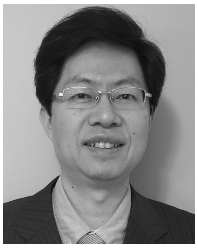

TAEHYUNG KIM (M'04–SM'12) received the Ph.D. degree in electrical engineering from Texas A&M University, College Station, TX, USA, in 2003. He was with the Digital Appliances Research Center, Samsung Electronics, as a Senior Research Engineer, in 2003. From 2004 to 2005, he was a Postdoctoral Researcher with the Advanced Vehicle, Power Electronics, and Motor Drive Laboratory, Texas A&M University. In 2005, he joined the Department of Electrical and Computer Engineering, University of Michigan-Dearborn, where he is currently an Associate Professor. In 2014, he visited Chung-Ang University as an invited Brain-Pool Research Scholar. His research interests include electric and hybrid electric vehicles, power electronics, and motor drives. He was a recipient of the 2012 Second Prize Paper Award from the IEEE Industry Applications Society (Annual Society's Best Magazine Article).